ChemComm

Accepted Manuscript

ROYAL SOCIETY OF CHEMISTRY

rsc.li/chemcomm

View Article Online
DOI: 10.1039/C9CC01825E

COMMUNICATION

Covalently functionalized carbon nanoparticles by a chiral Mn-Salen: a new nanocatalyst for enantioselective epoxidation of alkenes

Received 00th January 20xx,
Accepted 00th January 20xx

DOI: 10.1039/x0xx00000x

Agatino Zammataro,[a] Chiara Maria Antonietta Gangemi,[a] Andrea Pappalardo,[a,b] Rosa Maria Toscano,[a] Roberta Puglisi,[a] Giuseppe Nicotra,[c] Maria Elena Fragalà,[a] Nunzio Tuccitto[a,d] and Giuseppe Trusso Sfrazzetto*[a,b]

A new protocol to obtain Carbon Nanoparticles (CNPs) covalently functionalized with a chiral Mn-salen catalyst is here described. The new nanocatalyst (CNPs-Mn-Salen) was tested in the enantioselective epoxidation of some representative alkenes (CN-chromene, 1,2-dihydronapthalene and *cis*-β-ethyl styrene), obtaining better enantiomeric excess value respect to the catalyst single molecule, highlighting the role of the nanostructure in the enantioselectivity.

Olefin epoxidation is one of the most important and useful reaction due to the possibility to obtain a wide range of organic derivatives. This reaction found application in several technological fields.[1] In this context, chiral Mn(III)-salen derivatives play a central role due to the huge employment in the synthesis of chiral epoxides, which represent an important target for the pharmaceuticals and industries.[2-4] However, the exposure to transition metal ions, in particular manganese, at concentrations more than 5 mg/m^{-3}, can lead to important neurological disorders.[5] Therefore, many efforts have been devoted to reduce the amount of this metal ion into the catalytic systems. One of the most used strategy is to heterogenize the Jacobsen catalyst onto a solid surface.[6-13] Another strategy is to obtain nanocatalysts,[14] in which the amount of metal atoms is significantly reduced respect to the standard catalysts.

Carbon Nanoparticles (CNPs) are a new class of carbon nanomaterial, which display interesting photo-chemical and redox properties.[15] CNPs are nanoparticles about 10 nm of diameters, with a quasi-spherical shape. Due to their properties, including high optical and chemical stability, good water solubility, photobleaching resistance, biocompatibility and low cost, nowadays CNPs are successfully applied in a wide range of application fields, such as analytical,[16,17] biosensing,[18,19] bioimaging,[20,21] theranostic[22,23] molecular communication[24,25] and photocatalytic energy conversion.[26-28] However, very few examples of CNPs used as catalysts have been reported.[29-37] Among these, no example of catalyst for epoxidation has been described.

Although the one pot synthesis of CNPs is green, simple and versatile, the obtained CNPs derivatives do not display yet the properties reached by covalent functionalization of the external shell. Attractive hybrid approaches that combine the one-pot synthesis followed by covalent functionalization of the functional groups of the external shell may lead to a versatile and efficient preparation of new CNPs having different surface functionalities. Thus, decorating CNPs with a functional substrate/catalyst is a promising option to enhance their properties.

Here, the first example of covalent functionalization of CNPs with a chiral Mn-salen catalyst (**Mn-Salen-OH**, Scheme 1) is reported. The salen ligand has been functionalized in order to covalently react with carboxylic groups on the surface of the native CNPs, leading to an ester bond. The new nanostructure was tested as catalyst for the enantioselective epoxidation of alkenes, by using 1,2-dihydronaphtalene, CN-chromene and *cis*-β-ethyl styrene as model substrates. Scheme 1 shows the synthetic pathway to obtain catalyst **Mn-Salen-OH**. Salicylaldehyde was chloromethylated by using aqueous formaldehyde in hydrochloric acid, obtaining aldehyde **1** which, after reaction with $CuSO_4$ in DMSO/H_2O, was converted into 5-hydroxymethyl-2-hydroxy-benzaldehyde **2**.[38] The chiral salen ligand **4** was obtained by reaction of **2** with (*1R*,*2R*)-diphenyl-ethylendiamino-monochloride derivative **3**,[39-40] in the presence of triethylamine. Then, manganese was introduced into the salen ligand obtaining **Mn-Salen-OH** in almost quantitative yield.[41,42] All new compounds have been characterized by NMR and ESI-MS (see ESI†). The presence of hydroxylic group on the salen backbone allows to anchor this catalyst on the surface of native CNPs. These, in fact, contain several free carboxylic groups on their surface which, after activation, can react with **Mn-Salen-OH** leading to a stable

[a] Department of Chemical Sciences, University of Catania, Viale Andrea Doria 6, 95125, Catania, Italy. E-mail: giuseppe.trusso@unict.it
[b] INSTM Udr of Catania, Viale Andrea Doria 6, 95125, Catania, Italy.
[c] CNR-IMM, Zona industriale strada VIII, 5, 95121 Catania, Italy
[d] Laboratory for Molecular Surfaces and Nanotechnology (LAMSUN), Department of Chemical Sciences, University of Catania and CSGI, Italy.

† Electronic Supplementary Information (ESI) available: Synthetic procedures, characterization of compounds, NMR, ESI-MS, XPS spectra, SEM and TEM images. See DOI: 10.1039/x0xx00000x

covalent bond. Native CNPs were synthesized by hydrothermal decomposition.[24]

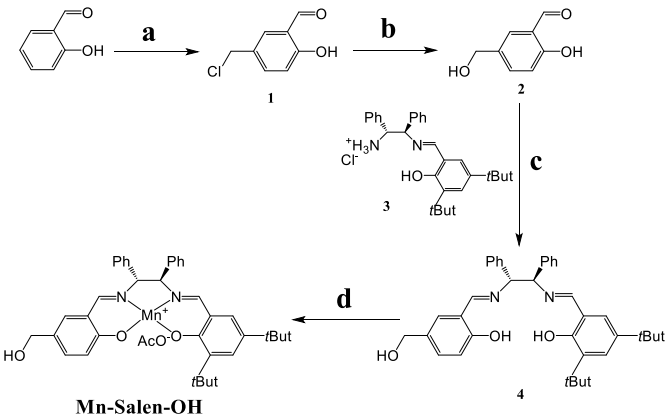

Scheme 1. Synthesis of **Mn-Salen-OH**. Reagents and conditions: a) formaldehyde (37% aqueous solution), concentrated HCl, 90 °C, 16h, 85%; b) $CuSO_4$, H_2O/DMSO (1/2), 110 °C, 2 h, 87%; c) Et_3N, EtOH, RT, 16h, 65%; d) $Mn(OAc)_3$, EtOH, RT, 16h, 95%.

The covalent functionalization of their surface is shown in Scheme 2. Carboxylic groups of CNPs (**CNPs-COOH**) were activated by using pentafluorophenol and EDAC x HCl (*N*-(3-Dimethylaminopropyl)-*N*′-ethylcarbodiimide hydrochloride), in solvolysis at 50°C overnight. The functionalized CNPs (**CNPs-PFF**) were purified by extraction in water/dichloromethane, due to the higher solubility in organic solvent respect to the starting **CNPs-COOH**. Then, reaction of **CNPs-PFF** with a large excess of **Mn-Salen-OH** leads to the nanocatalyst **CNPs-Mn-Salen**, which was purified by dialysis. **CNPs-Mn-Salen** has been characterized by ^{1}H NMR, XPS, TEM and SEM. In particular, ^{1}H NMR spectrum shows broad signals, according to the presence of manganese metal ion, in the region relative to the salen complex (see ESI†).

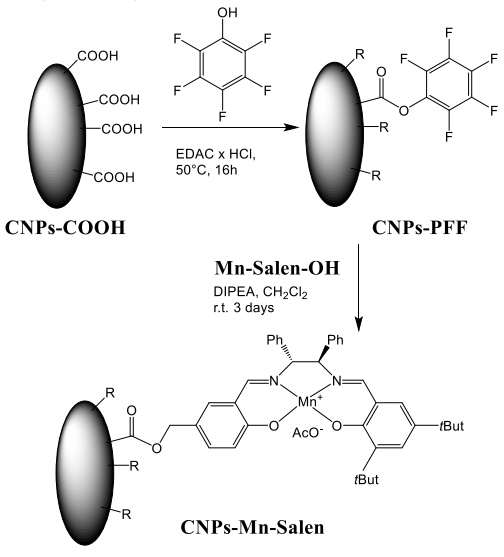

Scheme 2. Functionalization of CNPs with the chiral **Mn-Salen-OH**.

The XPS spectrum of the as prepared **CNPs-Mn-Salen** sample shows a C 1s band, at 285.0 eV (Figure S8, see ESI†), partially asymmetric due to chemical shift of C 1s related to carboxylate species having at higher binding energy.

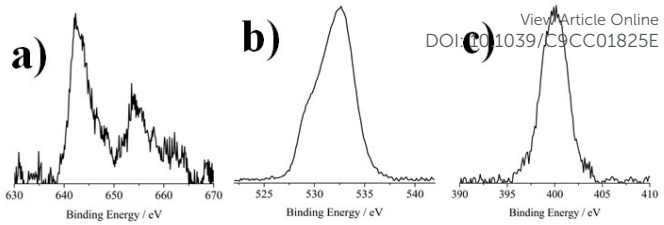

View Article Online
DOI: 10.1039/C9CC01825E

Figure 1. Al Kα excited XPS of the CNPs sample, measured in the a) Mn 2p, b) O 1s and c) N 1s binding energy region. Structure due to satellite radiation has been subtracted from the spectra.

Figure 1a shows the XPS Mn $2p_{3/2,½}$ spin-orbit components at 642.3 and 654.1 eV, partially overlapped with the high energy shake-up satellites typical of Mn(III) species,[12,13,43,44] while the XPS spectrum of the O 1s states for the **CNPs-Mn-Salen** sample shows two evident signals at 532.5 and 530.2 eV (Figure 1b). The first peak is largely due to the SiO_2 substrate, the shoulder at lower binding energy is assigned to chemical shift related to O-Mn and –COOH groups. Moreover, the XPS of **CNPs-Mn-Salen** sample in the N 1s binding energy region exhibits a signal at 400.0 eV (Figure 1c), since the Mn-salen complex possesses two imine groups.[12,13] Although XPS is a surface sensible analytical technique, since the diameter of the CNPs is smaller[24] than the sampling depth of the XPS, we assumed to probe the whole CNPs particle. Considering that the area of a **Mn-Salen** molecule is 1.4 nm^2,[13] we expect, in the case of complete surface coverage, 150 atoms of Mn per CNP having diameter of 7 nm. The XPS atomic concentration ratio C/Mn found is 195, corresponding to 55 atoms of Mn per CNP matching with a coverage of 33%. Taking into account the well-known adventitious carbon contamination, omnipresent in all air-exposed materials, the coverage is satisfactory in view of the catalytic purpose of such organic nanostructure.

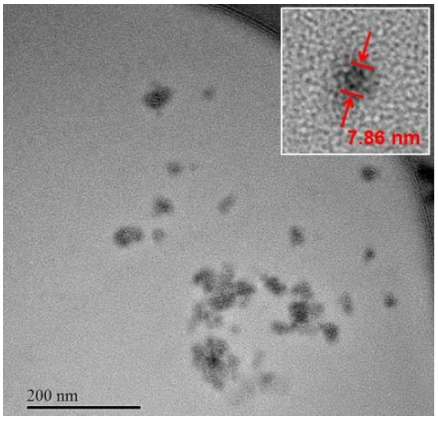

Figure 2. TEM BF-TEM acquired at 200KeV in low e dose, show the presence of small CNPs with an average size of 8nm.

TEM analysis reveals the presence of nanoparticles having an average diameter of 8 nm (Figure 2). Moreover, images taken at high resolution (HR-TEM, see ESI†, Fig. S11) reveal the presence of graphite-like carbon crystal structure in the nanoparticles core. The external shell around the CNPs is even visible as a slightly dark contrast around the core of the CNPs (inset of Figure 2). This is compatible with the presence of the functionalized complex anchored onto the CNPs' surface. SEM analysis is in good agreement with TEM results. SEM images

confirm the formation of carbon nanoparticles with dimension ranging from few nanometers (see ESI†, Fig. S10 red arrows) up to 20-40 nm. However, particles aggregation on substrate cannot be excluded during solvent evaporation.

Preliminary epoxidation results by using **CNPs-Mn-Salen** are shown in Table 1.

Table 1. Enantioselective epoxidation of 1,2-dihydronaphthalene, 6-CN-2,2-dimethylchromene and *cis*-β-ethyl styrene with NaClO catalyzed by **CNPs-Mn-Salen** in CH_2Cl_2 at 25 °C.[a]

Alkene	Entry	[**Nanocat.**] (mg/mL)[b]	Time (h)	e.e. (%)[c]	Conv. (%)[c]	TON[f] (TOF)[g]	C.B. (%)[h]
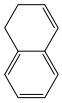	1	0.05	1	80[d]	10	8264 (8264)	97
	2	0.05	12	81[d]	12	9917 (4959)	95
	3	0.05	24	80[d]	15	12397 (1033)	94
	4	0.5	1	79[d]	35	2893 (2893)	95
	5	0.5	12	80[d]	49	4050 (337)	93
	6	0.5	24	80[d] (82)‡	50 (100)‡	4132 (172)	92 (97)‡
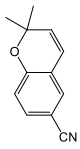	7	0.5	1	96[e]	18	1488 (1488)	96
	8	0.5	12	96[e]	29	2397 (200)	94
	9	0.5	24	95[e] (75)‡	30 (100)‡	2479 (103)	94 (96)‡

Alkene	Entry	Time (h)	e.e.$_{cis}$ e.e.$_{trans}$ (%)[c]	cis/trans	Conv. (%)[c]	TON[f] (TOF)[g]	C.B. (%)[h]
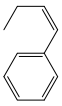	10[i]	1	71[d] 52[d]	7	59	4876 (4876)	97
	11[i]	12	71[d] 50[d]	7	65	5372 (448)	95
	12[i]	24	72[d] 50[d]	7	66	5455 (227)	95
	13‡	24	85[d] 59[d]	5	100	1176 (49)	97

[a] In all experiments [alkene] = [NaClO] =1.17 x 10^{-2} M, buffered with 1 mL of 0.05 M Na_2HPO_4 at pH 11.2 in a total volume of 2 mL; [b] stock solution of **CNPs-Mn-Salen** was prepared dissolving 5 mg of the nanocatalyst in 5 mL of CH_2Cl_2; [c]determined by GC analysis using a chiral column (see ESI†) and *n*-dodecane as internal standard; [d] config. (*1R,2R*) determined by measuring the optical rotation; [e] config. (*3R,4R*) determined by measuring the optical rotation; [f] TON = [overall products]/[catalyst]; [g] TOF = TON/reaction time (h); [h] Carbon Balance C.B. = (total carbon detected/total carbon feed);[45] [i] [**CNPs-Mn-Salen**] = 0.5 mg/mL.

1,2-dihydronaphtalene was chosen as substrate to setup the epoxidation conditions. In particular, by using a nanocatalyst concentration of 0.05 mg/mL, good enantiomeric excess but low conversion values were obtained (Table 1, entries 1-3). Increasing the concentration of **CNPs-Mn-Salen** (0.5 mg/mL) the conversion values have been increased (Table 1, entries 4-6). This setup was used with CN-chromene (Table 1, entries 7-9) and *cis*-β-ethyl styrene (Table 1, entries 10-12). In particular, with CN-chromene, conversion values are lower respect to those obtained with 1,2-dihydronaphtalene, but enantiomeric excess values are 95-96%, higher respect to those obtained with **Mn-Salen-OH**.‡ These results suggest that the presence of CNPs increase the enantiomeric excess, in the case of CN-chromene, although the conversion is low. The origin of the high enantioselectivity in the Jacobsen's epoxidation has been extensively studied,[46] but until now, not fully elucidated. The most common rationalization is attributed to the directions of approach of the alkene to the manganese active site (manganese-oxo). Cavallo and co-workers reported theoretical calculations that support this hypothesis.[47] More recently, a new justification about the origin of the enantioselectivity was proposed by Corey and coworkers.[48] In this hypothesis, the transition state assembly is slightly similar to a [3 + 2] cycloaddition between alkene and the catalyst. A possible explanation of the high enantioselectivity with CN-chromene can be ascribe to the chemical structure of this alkene. In particular, due to the presence of an oxygen atom in the fused ring system, some possible interactions can occur with the surface of the CNPs (e. g. H-bonding with some unfunctionalized groups) that reduce the reactivity, leading to low conversion values but, at the same time, increase the geometric constrains, thus obtaining high enantiomeric excess values.

Epoxidation reactions with *cis*-β-ethyl styrene show good conversion values after 1 hour (59%, Table 1, entry 10), higher respect to the other examined alkenes. This higher reactivity leaded to lower enantiomeric excess values (~71%, Table 2, entries 10-12) respect to the other substrates, as well as respect to the **Mn-Salen-OH** (Table 1, entry 13).‡ Furthermore, the [*cis*]/[*trans*] ratio (~7, with ~50% of e.e. values) suggests a short lifetime of the radical intermediate, invoked by Jacobsen and co-workers,[49] leading to the partial isomerization of the radical intermediate.

Recycling tests were performed by using 1,2-dihydronaphtalene as selected substrate (see ESI†, Fig. S9). **CNPs-Mn-Salen** can be recovered from the reaction media by extraction with CH_2Cl_2 (to remove the aqueous phase), and vacuum treatment at 100 °C for two hours (to remove the organic products/byproducts). After 4 cycles, the enantiomeric excesses remained almost unaltered, while conversion values decrease from 50% to 25%, suggesting a partial degradation of the nanocatalyst.

In summary, a new synthetic protocol for the covalent functionalization of CNPs was here reported. In particular, we anchored a chiral Mn-salen catalyst onto CNPs, leading to a new nanocatalyst able to catalyze the enantioselective epoxidation of some selected alkenes. This new catalytic system, using CN-chromene as substrate, permits to obtain chiral epoxides, with higher enantiomeric excess values respect to the molecular catalyst. We are still testing this nanocatalyst with other substrates in order to shed light on the origin of this enantioselectivity. Preliminary results revealed that the role of the nanostructure is essential in the increasing of enantioselectivity. Respect to the commercial catalysts used for the oxidation of organic substrates,[50] chiral Mn-Salen allows to control the enantioselectivity of the reaction. Furthermore, the functionalization of carbon

materials with Mn-Salen catalysts permits to reduce the amount of Mn in the reaction media and, in addition, to improve the stability of these nanocatalysts in alkaline conditions, required by the presence of NaClO as oxidant. Basic conditions, in fact, are harmful for the silica supports, which are largely used for the heterogenization of Jacobsen's catalysts.

The authors thank Prof. Antonino Gulino and Dr. Luca Spitaleri for XPS measurements. This work was supported by the University of Catania, Department of Chemical Sciences (Piano per la Ricerca 2016-2018– Linea Intervento 2).

Conflicts of interest

There are no conflicts to declare.

Notes and references

‡ Control reaction was performed by using [**Mn-Salen-OH**] = 8.50 x 10^{-4} M, [alkene] = [NaClO] = 1.17 x 10^{-2} M, buffered with 1 mL of 0.05 M Na_2HPO_4 at pH 11.2 in a total volume of 2 mL. With 1,2-dihydronaphtalene as substrate, after 24h, total conversion and 82% of enantiomeric excess were obtained. With CN-chromene as substrate, after 24h, total conversion and 75% of enantiomeric excess were obtained. With *cis*-β-ethyl styrene as substrate, after 24h, total conversion and 85% of enantiomeric excess were obtained.

1 C. Baleizão, *Chem. Rev.* 2006, **106**, 3987–4043
2 E. N. Jacobsen, E.N. Catalytic Asymmetric Synthesis; Ojima, I., Ed.; VCH:Weinheim, Germany, 1993; Chapter 4.2, pp. 159–202.
3 T. P. Yoon and E. N. Jacobsen, *Science* 2003, **299**, 1691–1693.
4 I. W. E. E Arends, *Angew. Chem. Int. Ed.* 2006, **45**, 6250–6252
5 R. M. Bowler, S. Nakagawa, M. Drezgic, H. A. Roels, R. M. Park, E. Diamond, D. Mergler, M. Bouchard, R. P. Bowler and W. Koller, *Neurotoxicology* 2007, **28**, 298–311.
6 J. M. Thomas and R. Raja, *Acc. Chem. Res.* 2008, **41**, 708–720.
7 J. R. Carey, S. K. Ma, T. D. Pfister, D. K. Garner, H. K. Kim, J. A. Abramite, Z. Wang, Z. Guo and Yi Lu *J. Am. Chem. Soc*. 2004, **126**, 10812–10813.
8 M. Pala and V. Ganesan, *Cat. Sci. Tech.* 2012, **2**, 2383–2388.
9 R. Raja, J. M. Thomas, M. D. Jones, B. F. G. Johnson and D. E. W. Vaughan, *J. Am. Chem. Soc.* 2003, **125**, 14982–14983.
10 C. Bianchini and P. Barbaro, *Top. Catal*. 2002, **19**, 17–32.
11 J. M. Fraile, J. I. Garcìa, C. I. Herrerìas, J. A. Mayoral and E. Pires, *Chem. Soc. Rev.* 2009, **38**, 695–706.
12 V. La Paglia Fragola, F. Lupo, A. Pappalardo, G. Trusso Sfrazzetto, R. M. Toscano, F. P. Ballistreri, G. Tomaselli and A. Gulino *J. Mater. Chem.* 2012, **22**, 20561–20565.
13 G. Trusso Sfrazzetto, S. Millesi, A. Pappalardo, R. M. Toscano, F. P. Ballistreri, G. A. Tomaselli and A. Gulino *Cat. Sci. Techn.* 2015, **5**, 673–679.
14 A. Agnoli, *Eur. J. Inorg. Chem.* 2018, 4311–4321.
15 F. R. Baptista, S. A. Belhout, S. Giordani and S. J. Quinn *Chem. Soc. Rev.* 2015, **44**, 4433—4453.
16 Y. M. Guo, Z. Wang, H. W. Shao and X. Y. Jiang *Carbon* 2013, **52**, 583–589.
17 S. N. Qu, H. Chen, X. M. Zheng, J. S. Cao and X. Y. Liu *Nanoscale* 2013, **5**, 5514–5518.
18 W. Shi, X. Li and H. Ma *Angew. Chem., Int. Ed.* 2012, **51**, 6432–6435.
19 A. W. Zhu, Q. Qu, X. L. Shao, B. Kong, Y. Tian, *Angew. Chem. Int. Ed.* 2012, **51**, 7185–7189.
20 S. T. Yang, L. Cao, P. J. G. Luo, F. S. Lu, X. Wang, H. F. Wang, M. J. Meziani, Y. F. Liu, G. Qi and Y. P. Sun *J. Am. Chem. Soc.* 2009, **131**, 11308–11309.
21 N. Licciardello, S. Hunoldt, R. Bergmann, G. Singh, C. Mamat, A. Faramus, J. L. Z. Ddungu, S. Silvestrini, M. Maggini, L. De Cola and H. Stephan *Nanoscale* 2018, **10**, 9880–9891.
22 L. Hu, Y. Sun, S. Li, X. Wang, K. Hu, L. Wang, X.-J. Liang and Y. Wu *Carbon* 2014, **67**, 508–513.
23 H. Wang, G. Cao, Z. Gai, K. Hong, P. Banerjee and S. Zhou *Nanoscale* 2015, **7**, 7885–7895.
24 N. Tuccitto, G. Li-Destri, G. M. L. Messina, G. Marletta *J. Phys. Chem. Lett.* 2017, **8**, 3861–3866.
25 N. Tuccitto, N., G. Li-Destri, G.M.L. Messina, G. Marletta, *PCCP* 2018, **20**, 30312–30320
26 V. Strauss, J. T. Margraf, C. Dolle, B. Butz, T. J. Nacken, J. Walter, W. Bauer, W. Peukert, E. Spiecker, T. Clark and D. M. Guldi *J. Am. Chem. Soc.* 2014, **136**, 17308–17316.
27 W. Tu, Y. Zhou and Z. Zou *Adv. Mater.* 2014, **26**, 4607–4626.
28 S. N. Habisreutinger, L. Schmidt-Mende and J. K. Stolarczyk *Angew. Chem. Int. Ed.* 2013, **52**, 7372–7408.
29 L.-M. Shen and J. Liu *Talanta* 2016, **156-157**, 245–256.
30 S. Muthulingam, I.-H. Lee and P. Uthirakumar *J. Colloid Interface Sci*. 2015, **455**, 101–109.
31 B. C. M. Martindale, G. A. M. Hutton, C. A. Caputo and E. Reisner *J. Am. Chem. Soc.* 2015, **137**, 6018–6025.
32 J. Briscoe, A. Marinovic, M. Sevilla, S. Dunn and M. Titirici *Angew. Chem. Int. Ed.* 2015, **54**, 4463–4468.
33 H. Li, C. Sun, M. Ali, F. Zhou, X. Zhang and D. R. MacFarlane *Angew. Chem. Int. Ed.* 2015, **54**, 8420–8424.
34 D. Mosconi, D. Mazzier, S. Silvestrini, A. Privitera and C. Marega *ACS. Nano* 2015, **9**, 4156–4164.
35 S. Zhao, C. Li, J. Liu, N. Liu, S. Qiao, Y. Han, H. Huang, Y. Liu and Z. Kang *Carbon* 2015, **92**, 64–73.
36 J.-J. Zhang, Z.-B. Wang, C. Li, L. Zhao, J. Liu, L.-M. Zhang and D.-M. Gu *J. Power Sources* 2015, **289**, 63–70.
37 Y. Jin, C. Hu, Q. Dai, Y. Xiao, Y. Lin, J. W. Connell, F. Chen and L. Dai *Adv. Funct. Mater.* 2018, **28**, 1804630–1804637.
38 A. Gulino, G. Trusso Sfrazzetto, S. Millesi, A. Pappalardo, G. A. Tomaselli, F. P. Ballistreri, R. M. Toscano and L. Fragalà *Chem. Eur. J.* 2017, **23**, 1576–1583.
39 A. Pappalardo, M. E. Amato, F. P. Ballistreri, G. A. Tomaselli, R. M. Toscano and G. Trusso Sfrazzetto *J. Org. Chem.* 2012, **77**, 7684–7687.
40 A. D'Urso, C. Tudisco, F. P. Ballistreri, G. G. Condorelli, R. Randazzo, G. A. Tomaselli, R. M. Toscano, G. Trusso Sfrazzetto and A. Pappalardo *Chem. Commun.* 2014, **50**, 4993–4496.
41 F. P. Ballistreri, C. M. A. Gangemi, A. Pappalardo, G. A. Tomaselli, R. M. Toscano and G. Trusso Sfrazzetto *Int. J. Mol. Sci.* 2016, **17**, 1112–1120.
42 A. Patti, S. Pedotti, F. P. Ballistreri and G. Trusso Sfrazzetto *Molecules*, 2009, **14**, 4312–4325.
43 D. Q. Li, B. I. Swanson, J. M. Robinson and M. A. Hoffbauer, *J. Am. Chem. Soc.*, 1993, **115**, 6975–6980.
44 M. C. Biesinger, B. P. Payne, A. P. Grosvenor, L. W. M. Lau, A. R. Gerson and R. S. C. Smart *Appl. Surf. Sci.* 2011, **257**, 2717–2730.
45 M. S. C. Chan, E. Marek, S. A. Scott and J. S. Dennis *J. Catal*. 2018, **359**, 1–7.
46 T. Katsuki, *Coord. Chem. Rev.* 1995, **140**, 189–214.
47 H. Jacobsen and L. Cavallo *Chem. A Eur. J.* 2001, **7**, 800–807.
48 L. Kurti, M. M. Blewett and E. J. Corey *Org. Lett.* 2009, **11**, 4592–4595.
49 W. Zhang, N. H. Lee and E. N. Jacobsen *J. Am. Chem. Soc.* 1994, **116**, 425–426.
50 R. A. F. Tomás, J. C. M. Bordado and J. F. P. Gomes *Chem. Rev.*, 2013, **113**, 7421–7469.

Covalently functionalized carbon nanoparticles by a chiral Mn-Salen: a new nanocatalyst for enantioselective epoxidation of alkenes

Agatino Zammataro, Chiara Maria Antonietta Gangemi, Andrea Pappalardo, Rosa Maria Toscano, Roberta Puglisi, Nunzio Tuccitto, Giuseppe Trusso Sfrazzetto

The first nanocatalyst, obtained *via* "step-by-step" functionalization of CNPs, for enantioselective epoxidation of non-functionalized alkenes is here reported